PAPER

Check for updates

Vitamin B$_6$ cofactor-directed fluorescent "turn-on" detection of alkaline-phosphatase activity using bovine serum albumin-functionalized Mn–ZnS quantum dots†

Sonkeshriya Dhanshri and Suban K Sahoo [iD] *

We introduced a simple approach for the fluorescent "turn-on" detection of alkaline phosphatase (ALP) activity. We employed bovine serum albumin (BSA)-functionalized manganese-doped zinc sulfide (Mn–ZnS) quantum dots (QDs) and the phosphate substrate was the vitamin-B$_6$ cofactor pyridoxal 5'-phosphate (PLP). The emission of Mn–ZnS QDs at 604 nm was quenched in the presence of PLP due to formation of an imine linkage between the free amine groups present in functionalized BSA and aldehyde group of PLP. Such fluorescence quenching was not observed with other cofactors of vitamin B$_6$, such as pyridoxal, pyridoxamine, or pyridoxine. ALP catalyzes a dephosphorylation reaction in biological processes, where it can convert albumin-bound PLP into pyridoxal. Mimicking this biological process, the PLP-directed quenched fluorescence of QDs was restored upon ALP addition. The developed nanoprobe showed a limit of detection of ALP of 0.003 U L^{-1}. We applied this nanoprobe for the monitoring of ALP activity in biological (human serum and plasma) samples.

1. Introduction

In recent years, owing to their wide applications in healthcare and diagnosis, research on fluorescence sensing and biosensing has flourished. Alkaline phosphatase (ALP) is an important enzyme used as a biomarker for the diagnosis of various diseases. Therefore, detection of ALP activity has become important in biosensing.[1] Fluorescence-based approaches for ALP detection have garnered attention due to their simplicity, cost-effectiveness, rapidity, and high sensitivity.[1,2] ALP is a glycoprotein-bound dimeric enzyme that catalyzes dephosphorylation reactions at high pH by hydrolysis. It is distributed mainly in the liver, bones and kidneys.[3] The main function of ALP as a membrane-bound enzyme is to remove phosphate groups from proteins, nucleic acids, and small molecules.[4–6] The mean ALP concentration in the human body is about 20–140 U L^{-1}.[1] An abnormal level of ALP can cause hypophosphatasia, neurological disorders, liver dysfunction, as well as carcinomas.[7] Therefore, several fluorescent based "turn-off" and "turn-on" sensors have been reported for the detection of ALP activity.[8–14] The turn-on strategy is very popular thanks to its high sensitivity and ability to avoid false-positive signals.[1]

A fluorescent chemosensor can be designed by suitably connecting a light-emitting unit with an analyte-binding site. The light-emitting unit may be an organic fluorophore or a fluorescent nanomaterial. Use of fluorescent nanomaterials has aided sensing and biosensing owing to their excellent optoelectronic properties: narrow and symmetric emission spectra, high quantum yield, photostability, and large Stokes shift.[15,16] Among various fluorescent nanomaterials,[17–20] semiconductor quantum dots (QDs) have been applied extensively for sensor development with potential utility for *in vivo* and *in vitro* imaging due to their extraordinary size-dependent photoluminescence.[21–25] However, application of semiconductor QDs in sensing and bioimaging is hampered by toxicity due to the use of heavy metals such as Cd and Pb.[26] Alternately, manganese-doped zinc sulfide quantum dots (Mn–ZnS QDs) have drawn wide attention for the design of fluorescent sensors due to their low toxicity, strong phosphorescence emission, long lifetime, and stable wide bandgap.[27–31] In the present study, bovine serum albumin-capped manganese-doped zinc sulfide quantum dots (BSA-Mn–ZnS QDs) were synthesized and applied for the cascade detection of vitamin B$_6$ cofactor pyridoxal 5'-phosphate (PLP) and the enzymatic activity of ALP.

Department of Chemistry, Sardar Vallabhbhai National Institute of Technology, Surat-395007, Gujarat, India. E-mail: sks@chem.svnit.ac.in, suban_sahoo@rediffmail.com; Tel: +91 9723220556
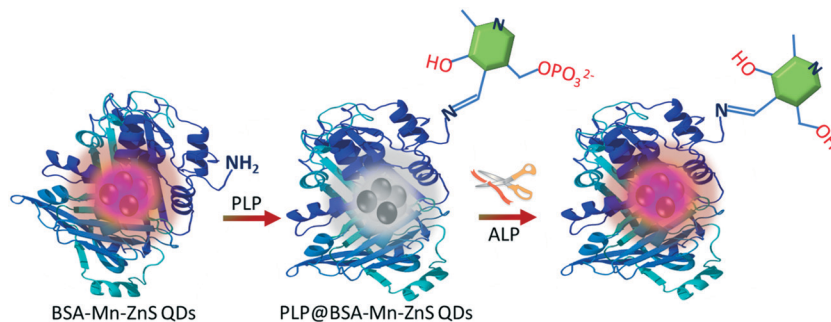
Scheme 1 Sequential detection of PLP and ALP using BSA-capped Mn–ZnS QDs (schematic).

The emission of BSA-capped Mn–ZnS QDs was quenched upon interaction with PLP (Scheme 1). BSA is a globular non-glycoprotein, contains 583 amino acid residues, and has 17 cysteine residues (eight disulfide bridges and one free thiol group).[32] BSA contains major functional groups (amine, hydroxyl, thiol, and carboxyl) and its biocompatibility is convenient for QD synthesis.[33,34] The free amine group of the functionalized BSA of Mn–ZnS QDs interacted with PLP by forming an imine linkage and quenched the emission of BSA-capped Mn–ZnS QDs. PLP is the most active form of vitamin B6.[35] An inadequate amount of PLP at the intracellular level can cause autism, schizophrenia, Alzheimer's disease, Parkinson's disease, or epilepsy.[36,37] Albumin-bound PLP in the liver acts as a "reservoir" for pyridoxal (PL), and can cross cell membranes only if ALP can catalytically convert PLP into PL.[38] Mimicking this biological process, when ALP was added to PLP-decorated BSA-Mn–ZnS QDs, the dephosphorylation of PLP to PL resulted, which restored the emission of QDs.

2. Experimental

2.1. Reagents and instrumentation

BSA, ALP, adenosine monophosphate (AMP), adenosine diphosphate (ADP), adenosine triphosphate (ATP), glutathione (GSH), cysteine (Cyst), homocysteine (Hcyst), zinc acetate (Zn (Ac)$_2$·2H$_2$O), manganese chloride (MnCl$_2$), sodium sulfide (Na$_2$S.9H$_2$O), tris(hydroxymethyl)aminomethane, and vitamin-B$_6$ cofactors, such as PLP, pyridoxamine (PYOA), pyridoxine (PY), and PL, were obtained from MilliporeSigma. All solutions were prepared using water obtained from MilliporeSigma.

Fluorescence spectroscopy was done on a Cary Eclipse fluorescence spectrophotometer (Agilent Technologies) adjusted with a slit width for an excitation wavelength and emission wavelength of 10 nm and 20 nm, respectively. The fluorescence range of spectra was recorded from 310 nm to 800 nm by excitation of the sample at 300 nm. A Varian Cary 50 spectrophotometer (Agilent Technologies) was used to record UV-vis spectra in the range 200–800 nm. UV-vis spectra were recorded using a quartz cuvette of path length 1 cm. Each cuvette contained ≥2 mL of sample solution, and was used to record absorption and fluorescence spectra. The

Fourier transform-infrared (FT-IR) spectra were recorded using IRAffinity-1S (Shimadzu).

2.2. Preparation of BSA-Mn–ZnS QDs

BSA-Mn–ZnS QDs were synthesized and characterized by a procedure reported previously.[39] In brief, to 5 mL of an aqueous solution of BSA (250 mg mL^{-1}) was added (dropwise) 1250 μL of aqueous Zn(Ac)$_2$·2H$_2$O (0.1 M) and 250 μL of an aqueous solution of MnCl$_2$ (0.5 M) with constant stirring for 30 min. To this mixture was added (dropwise) 1250 μL of Na$_2$S·9H$_2$O (0.1 M) under constant stirring. The resulting QDs solution was stirred for an additional 60 min. The obtained colloidal BSA-Mn–ZnS QDs solution was stored under room temperature for sensing studies.

2.3. Procedure for sensing experiments

A 2 mL working solution of the probe was prepared by diluting 15 μL of BSA-Mn–ZnS QDs from the stock solution with 1985 μL of water. Vitamin-B$_6$ cofactors (PYOA, PY, PL, and PLP; 45 μL, 1 × 10^{-3} M) were added to the probe to investigate selectivity. The fluorescence study revealed that PLP quenched the fluorescence of QDs selectively. A fluorescence titration was undertaken by adding incremental amounts of PLP from 0 M to 2.68 × 10^{-5} M to the QDs solution. The slope of the calibration curve was used to calculate the limit of detection (LOD) by applying the International Union of Pure and Applied Chemistry-approved equation LOD = 3 α/slope, where α is the relative standard deviation (RSD) of the fluorescence reading of 10 blank samples.

The catalytic activity of ALP was examined using buffer solutions (phosphate, carbonate–bicarbonate, and Tris-HCl). A suitable activity of ALP was shown in 0.1 M Tris-HCl buffer (pH = 8.0). A stock solution of ALP was prepared by taking 1 mg of ALP in 1 mL of buffer to obtain a concentration of 1 mg mL^{-1}. Furthermore, 100 μL of the ALP stock solution was diluted to 10 mL with Tris-HCl buffer to obtain a concentration of 0.01 mg mL^{-1} of ALP. The ALP-probe solution was prepared by adding PLP (45 μL, 1 × 10^{-3} M) to a solution of BSA-Mn–ZnS QDs prepared by diluting 15 μL from the stock solution with 1985 μL of buffer. To investigate selectivity and interference, different bioactive analytes (10
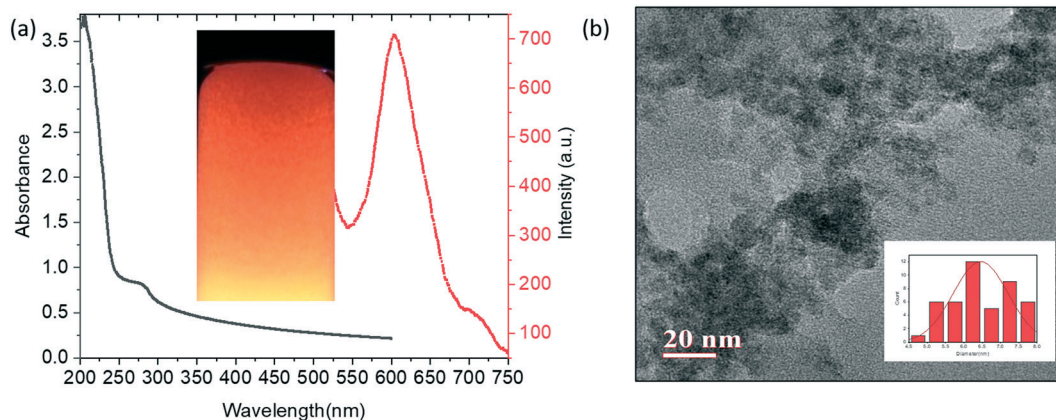
Fig. 1 (a) UV-vis absorption and emission spectra (λ_{exc} = 310 nm) of BSA-Mn–ZnS QDs (inset shows an image of a QDs solution irradiated with $UV_{365\ nm}$ light). (b) Transmission electron micrograph of BSA-capped Mn-doped ZnS QDs.

μL, 1×10^{-3} M) prepared fresh in water (Millipore) and ALP (10 μL, 0.047 U L^{-1}) were added to a solution of the probe PLP@BSA-Mn–ZnS QDs followed by incubation for 30 min at 37 °C. Batch fluorescence titration of PLP@BSA-Mn–ZnS QDs was carried out by incremental addition of ALP, and spectra were recorded after 30 min of incubation.

ALP activity was monitored in human plasma and serum to check the practical utility of the probe PLP@BSA-Mn–ZnS QDs. The samples of human serum and plasma were collected with consent from donors and all relevant guidelines were followed. Samples were centrifuged at 10 000 rpm for ~10 min and maintained to neutral pH. Samples were diluted 10 times before spiking with a known amount of ALP. Spiked samples were added to the probe solution followed by incubation for 30 min. Then, spectra were recorded to obtain the found concentration of ALP. Percentage recovery was calculated by comparing the added concentration and found concentration of ALP.

3. Results and discussion

3.1. PLP detection

A procedure reported previously was adopted to synthesize BSA-capped Mn–ZnS QDs with some minor modifications.[39] BSA-Mn–ZnS QDs showed a flat and broad absorption from 250 nm to 600 nm with an absorption maxima at 278 nm. An emission band centered at 604 nm (λ_{exc} = 310 nm) appeared due to the electronic transition from $^4T_1$ to $^6A_1$ of doped Mn (Fig. 1a). The transmission electron micrograph of the QDs revealed the formation of spherical and well-dispersed particles of diameter ~6 nm (Fig. 1b). The FT-IR spectra of BSA and BSA-Mn–ZnS QDs were recorded and compared to support the functionalization of BSA over the surface of QDs (Fig. S1†). With some variations, the bands of BSA alone were observed in BSA-Mn–ZnS QDs. A broad band at 3500–3100 cm^{-1} appeared due to the stretching vibration of hydroxy and amine groups. Bands between 1650 cm^{-1} and 1500 cm^{-1} due

to the amide bond supported the functionalization of BSA over the surface of QDs.

The strong orange emission from QDs was used to study the interaction of functionalized BSA with cofactors of vitamin B_6 (PLP, PL, PYOA, and PY). As shown in Fig. 2, the emission intensity of BSA-Mn–ZnS QDs at 604 nm was quenched in the presence of PLP. Other cofactors of vitamin B_6 (PL, PYOA, and PY) failed to perturb the fluorescence profile of QDs. Post-functionalization of PLP over the surface of QDs followed by photoinduced electron transfer (PET) from the excited conduction band of QDs to the lowest unoccupied molecular orbital (LUMO) of PLP is expected to quench fluorescence at 604 nm.[40,41] The free amine groups of BSA were expected to form an imine linkage with the aldehyde group of PLP. The FT-IR spectra of PLP@BSA-Mn–ZnS QDs showed a vibration at 1648 cm^{-1}, which supported the formation of an imine linkage between PLP and functionalized BSA (Fig. S1b†). Furthermore, X-ray photoelectron spectroscopy (XPS) of BSA-Mn–ZnS QDs was
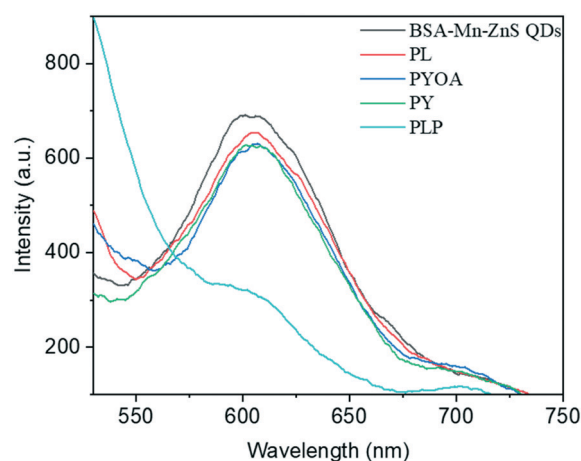

Fig. 2 Changes in fluorescence spectra of BSA-Mn–ZnS QDs in the presence of different cofactors of vitamin B_6 (2.25×10^{-5} M).
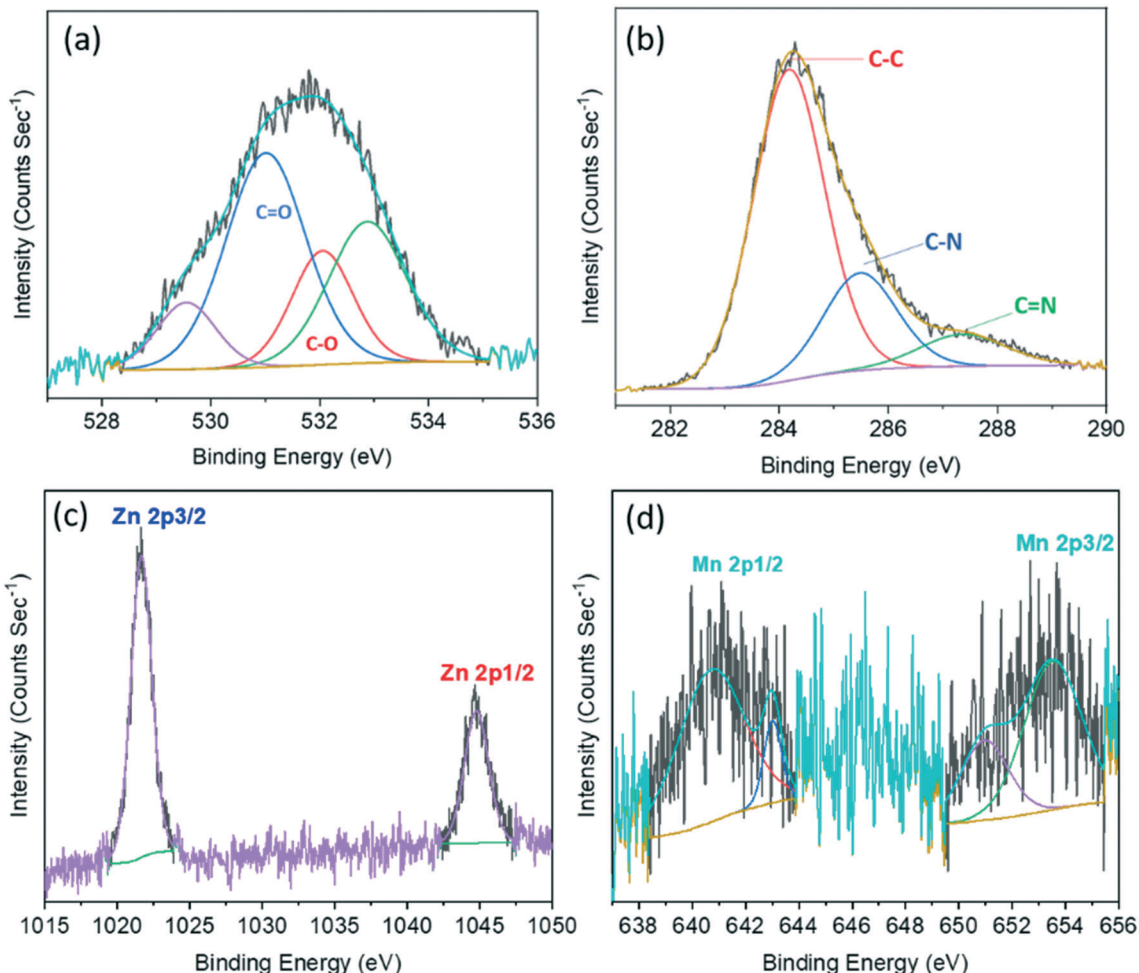
Fig. 3 XPS deconvoluted spectra of PLP@BSA-Mn–ZnS QDs for C 1s showing the characteristic spectrum for C=O and C–O (a), C–C, C–N, and C=N (b), Zn 2p (c), and Mn 2p (d).

undertaken in the presence of PLP to obtain a deeper insight into the interaction between PLP and BSA-Mn–ZnS QDs (Fig. S2 and 3). Deconvolution of some important elements in the XPS survey spectrum supported formation of an imine linkage. The C 1s peak was deconvoluted into two components (Fig. 3a): the peak at 531.4 eV was attributed to the C–O and C=O of the monodentate carboxylate group and the peak at 532.1 eV was assigned to the bidentate carboxylate.[42] The C1s peak consists of other sub-bands of C–C, C–N, and C=N at 284.14, 285.49, and 287.47 eV, respectively.[43] The deconvoluted Mn peak showed bands at 640.79 eV and 653.54 eV for Mn 2p1/2 and Mn 2p3/2, respectively (Fig. 3c). For Zn, it splits into Zn 2p3/2 (peak at 1021.64 eV) and Zn 2p1/2 (peak at 1044.68 eV).[44]

PLP has an active role in biological processes. Hence, the detection and quantification of PLP is important because PLP is used as a biomarker for the diagnosis of various diseases.[35,45] Therefore, the sensitivity of the probe BSA-Mn–ZnS QDs was examined by carrying out fluorescence titration (Fig. S3a†): an aliquot of PLP was added successively to the solution of BSA-Mn–ZnS QDs and, after each addition,

spectra were recorded. The fluorescence intensity at 604 nm of QDs decreased continuously with an increasing concentration of PLP. The change in fluorescence intensity of QDs at 604 nm showed good linearity from 4.9 μM to 22.1 μM of PLP. Using the slope of the calibration curve (Fig. S3b†), the PLP concentration could be estimated down to 1 μM. The sensitivity of QDs for PLP was comparable with that reported for fluorescence-based sensors. Also, the developed probe BSA-Mn–ZnS QDs avoids the toxic reagents (*e.g.*, chlorite, bisulfate, and cyanide) used for PLP detection by various analytical approaches.[23]

3.2. Detection of ALP activity

ALP belongs to a class of hydrolases and acts on phosphate groups. This enzyme catalytically dephosphorylates the albumin-bound PLP into PL. In the present study, PLP could quench the emission of BSA-Mn–ZnS QDs at 604 nm but was unaffected in the presence of PL. The distinct fluorescence changes of BSA-Mn–ZnS QDs in the presence of PLP and PL encouraged us to develop an ALP nanoprobe. A 2 mL solution

of an ALP nanoprobe, PLP@BSA-Mn–ZnS QDs, was prepared by mixing 45 μL of PLP (1×10^{-3} M) with BSA-Mn–ZnS QDs solution. The pH was adjusted at 8.0 with Tris-HCl as the buffer. ALP (10 μL, 0.047 U L^{-1}) and other bioactive analytes (10 μL, 1×10^{-3} M) were introduced to the PLP@BSA-Mn–ZnS QDs solution, followed by incubation at 37 °C for 30 min, before recording the fluorescence spectra. The quenched emission of QDs at 604 nm was enhanced selectively in the presence of ALP (Fig. 4a). Other analytes showed no noticeable changes in the fluorescence profile of PLP@BSA-Mn–ZnS QDs. This result supported the notion of ALP-driven catalytic dephosphorylation of PLP into PL.[46] This phenomenon is expected to suppress PET from the excited conduction band of QDs to the LUMO of PL and enhance the fluorescence intensity at 604 nm.

The specificity of PLP@BSA-Mn–ZnS QDs for ALP detection was inspected under a competitive environment (Fig. 4b). The fluorescence spectra of PLP@BSA-Mn–ZnS QDs were recorded in the presence of ALP (10 μL,

0.047 U L^{-1}) and co-presence of different interfering bioactive analytes (10 μL, 1×10^{-3} M). The ALP-driven fluorescence enhancement of PLP@BSA-Mn–ZnS QDs was practically unaltered in the presence of other bioactive analytes. These outcomes confirmed the high selectivity of the nanoprobe PLP@BSA-Mn–ZnS QDs for detecting ALP activity.

The catalytic activity of ALP could restore the quenched emission of PLP@BSA-Mn–ZnS QDs by converting PLP into PL under the optimized conditions of Tris-HCl as buffer (pH = 8.0) and 30 min of incubation at 37 °C. Batch fluorescence titration was undertaken to examine the sensitivity of PLP@BSA-Mn–ZnS QDs as an ALP probe (Fig. 5a). For the titration, a 2 mL solution of the nanoprobe PLP@GSH-Mn–ZnS QDs was placed in different vials and incremental amounts of ALP (1 μL) were added. The recorded fluorescence spectra showed continuous enhancement at 604 nm with increasing amounts of ALP. The titration data were used to plot a calibration graph by taking the changes in fluorescence intensity at 604 nm from 0.005 U L^{-1} to 0.047 U
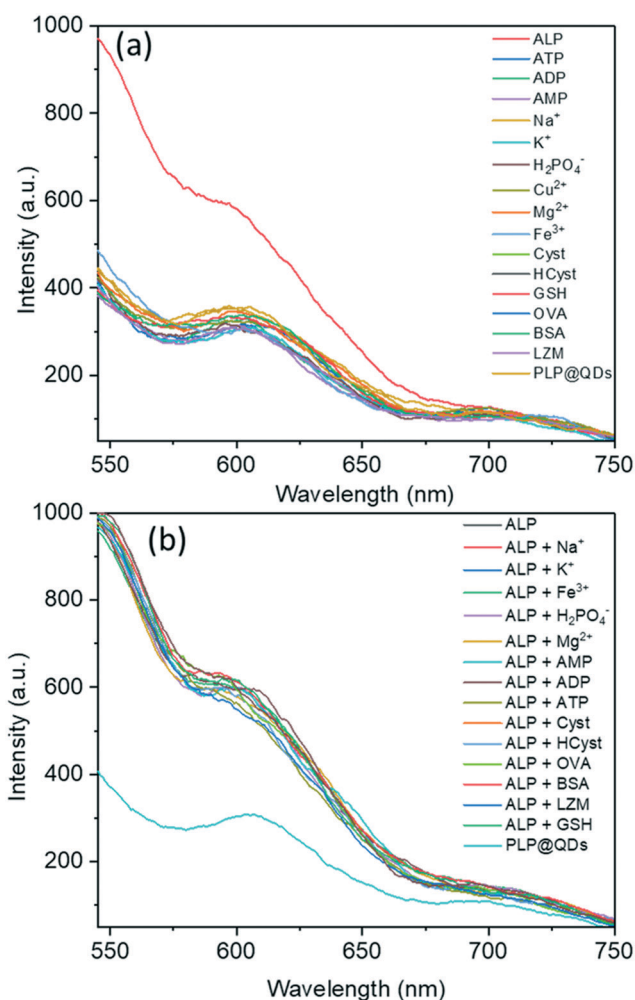

Fig. 4 Fluorescence spectra of PLP@BSA-Mn–ZnS QDs in the presence of various bioactive analytes (a). Fluorescence spectra of PLP@BSA-Mn–ZnS QDs in the presence of ALP and other interfering bioactive analytes (b).
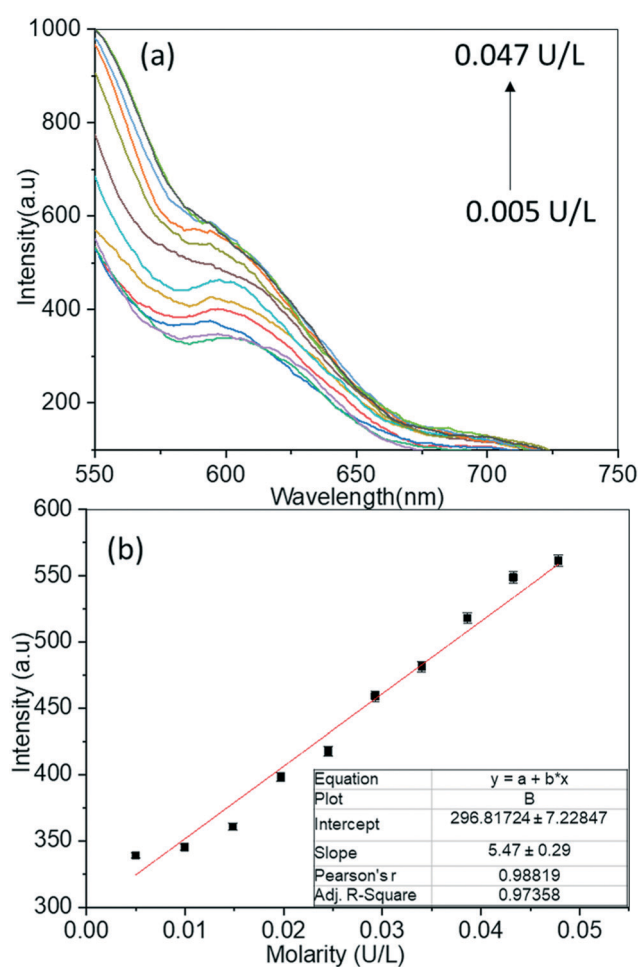

Fig. 5 Changes in fluorescence spectra of PLP@BSA-Mn–ZnS QDs with increasing amounts of ALP (a), and the calibration curve used to estimate ALP sensitivity (b).

Table 1 Analyses of real samples to quantify ALP activity using the nanoprobe PLP@BSA-Mn–ZnS QDs

Samples	Found (U L^{-1})	Added (U L^{-1})	Recovery%	RSD% ($n = 3$)
Plasma	0.098	0.099	99	1.31
	0.440	0.430	103	0.80
Serum	0.210	0.240	90	2.05
	0.477	0.470	101	1.02

L^{-1} (Fig. 5b), and LOD was estimated to be 0.003 U L^{-1}. The ALP level in blood of a healthy adult is 20–140 U L^{-1}.[1,2] The developed nanoprobe showed a much lower LOD and was analytically comparable/superior to that of reported fluorescent ALP probes.[1]

ALP activity was monitored on human serum and plasma samples to examine the practicality of the developed nanoprobe PLP@GSH-Mn–ZnS QDs. Diluted samples of human serum and plasma were spiked with a standard solution of ALP, and then the PLP@GSH Mn–ZnS QDs solution was added. Fluorescence spectra were recorded at 604 nm to determine the ALP concentration. The nanoprobe PLP@BSA-Mn–ZnS QDs showed satisfactory recovery (Table 1), which suggested good practicability for quantifying ALP activity in biological samples.

4. Conclusions

BSA-stabilized Mn–ZnS QDs were synthesized and applied for the cascade detection of PLP and ALP activity. The fluorescence intensity of BSA-Mn–ZnS QDs at 604 nm was quenched in the presence of PLP with a sensitivity of 1 μM. PLP was expected to form an imine linkage with the free amine group in the functionalized BSA in Mn–ZnS QDs. Furthermore, PLP@BSA-Mn–ZnS QDs were applied for fluorescent turn-on detection of ALP. In the presence of ALP, PLP@BSA-Mn–ZnS QDs aided catalytic dephosphorylation of albumin-bound PLP and were converted into PL@BSA-Mn–ZnS QDs. The quenched fluorescence at 604 nm was enhanced upon conversion of PLP into PL, which allowed ALP detection down to 0.003 U L^{-1}. Importantly, the applicability of PLP@BSA-Mn–ZnS QDs was validated by monitoring ALP activity in real biological (human serum and plasma) samples.

Conflicts of interest

There are no conflicts to declare.

References

1 Y. Han, J. Chen, Z. Li, H. Chen and H. Qiu, *Biosens. Bioelectron.*, 2020, **148**, 111811.

2 Z. Song, Y. Hong, R. T. Kwok, J. W. Lam, B. Liu and B. Z. Tang, *J. Mater. Chem. B*, 2014, **2**, 1717–1723.

3 U. Sharma, D. Pal and R. Prasad, *Indian J. Clin. Biochem.*, 2014, **29**, 269–278.

4 S. Liu, X. Wang, S. Pang, W. Na, X. Yan and X. Su, *Anal. Chim. Acta*, 2014, **827**, 103–110.

5 J. Chen, H. Jiao, W. Li, D. Liao, H. Zhou and C. Yu, *Chem. – Asian J.*, 2013, **8**, 276–281.

6 H. Zhang, Q. Ju, S. Pang, N. Wei and Y. Zhang, *Dyes Pigm.*, 2021, **194**, 109569.

7 X. Zhou, F. Y. Khusbu, H. Chen and C. Ma, *Talanta*, 2020, **208**, 120453.

8 Y. Zhang, Y. Nie, R. Zhu, D. Han, H. Zhao and Z. Li, *Talanta*, 2019, **204**, 74–81.

9 J. Zhang, X. Lu, Y. Lei, X. Hou and P. Wu, *Nanoscale*, 2017, **9**, 15606–15611.

10 X. Han, M. Han, L. Ma, F. Qu, R.-M. Kong and F. Qu, *Talanta*, 2019, **194**, 55–62.

11 P. Ni, C. Chen, Y. Jiang, C. Zhang, B. Wang, B. Cao, C. Li and Y. Lu, *Sens. Actuators, B*, 2019, **301**, 127080.

12 Y. Zhang, Y. Li, C. Zhang, Q. Zhang, X. Huang, M. Yang, S. A. Shahzad, K. K.-W. Lo, C. Yu and S. Jiang, *Anal. Bioanal. Chem.*, 2017, **409**, 4771–4778.

13 X. L. Hu, X. M. Wu, X. Fang, Z. J. Li and G. L. Wang, *Biosens. Bioelectron.*, 2016, **77**, 666–672.

14 L. Hu, Q. Zhang, X. Gan, S. Lin, S. Han and Z. Zhang, *Microchim. Acta*, 2018, **185**, 1–6.

15 S. K. Sahoo, *Sensing and biosensing with optically active nanomaterials*, Elsevier, 2022.

16 X. Liang, H. Wang, Y. Zhu, R. Zhang, V. C. Cogger, X. Liu, Z. P. Xu, J. E. Grice and M. S. Roberts, *ACS Nano*, 2016, **10**, 387–395.

17 J.-G. You, C.-Y. Lu, A. S. K. Kumar and W.-L. Tseng, *Nanoscale*, 2018, **10**, 17691–17698.

18 Y. Zhong, F. Xue, P. Wei, R. Li, C. Cao and T. Yi, *Nanoscale*, 2018, **10**, 21298–21306.

19 H. Fan, K. Dukenbayev, Q. Sun, M. Khamijan, A. Turdaliyev, A. Ysmaiyl, A. Tassanbiyeva, C. Ma and Y. Xie, *RSC Adv.*, 2021, **11**, 33253–33259.

20 V. Bhardwaj, S. A. Kumar and S. K. Sahoo, *ACS Appl. Bio Mater.*, 2020, **3**, 7021–7028.

21 D. Bera, L. Qian, T.-K. Tseng and P. H. Holloway, *Materials*, 2010, **3**, 2260–2345.

22 M. J. Molaei, *RSC Adv.*, 2019, **9**, 6460–6481.

23 M. J. Molaei, *Talanta*, 2019, **196**, 456–478.

24 V. Pandey, V. K. Tripathi, K. K. Singh, T. Bhatia, N. K. Upadhyay, B. Goyal, G. Pandey, I. Hwang and P. Tandon, *RSC Adv.*, 2019, **9**, 28510–28524.

25 S. Jin, Y. Hu, Z. Gu, L. Liu and H.-C. Wu, *J. Nanomater.*, 2011, **2011**, 834139.

26 P. Wu and X.-P. Yan, *Chem. Soc. Rev.*, 2013, **42**, 5489–5521.

27 S. Kayal and M. Halder, *Analyst*, 2019, **144**, 3710–3715.

28 X. Fang, T. Zhai, U. K. Gautam, L. Li, L. Wu, Y. Bando and D. Golberg, *Prog. Mater. Sci.*, 2011, **56**, 175–287.

29 J. Patel, B. Jain, A. K. Singh, M. A. B. H. Susan and L. Jean-Paul, *Microchem. J.*, 2020, **155**, 104755.

30 H. Yang, S. Santra and P. H. Holloway, *J. Nanosci. Nanotechnol.*, 2005, **5**, 1364–1375.

31 E. Sotelo-Gonzalez, L. Roces, S. Garcia-Granda, M. T. Fernandez-Arguelles, J. M. Costa-Fernandez and A. Sanz-Medel, *Nanoscale*, 2013, **5**, 9156–9161.

32 Q. Zhang, Y. Ni and S. Kokot, *Spectrosc. Lett.*, 2012, **45**, 85–92.

33 A. Papadopoulou, R. J. Green and R. A. Frazier, *J. Agric. Food Chem.*, 2005, **53**, 158–163.

34 H. Li and X. Yang, *Anal. Methods*, 2015, **7**, 8445–8452.

35 M. L. di Salvo, M. K. Safo and R. Contestabile, *Front. Biosci., Elite Ed.*, 2012, **4**, 897–913.

36 C. Chauhan, V. Bhardwaj and S. K. Sahoo, *Microchem. J.*, 2021, 106778.

37 D. Diaz-Diestra, B. Thapa, J. Beltran-Huarac, B. R. Weiner and G. Morell, *Biosens. Bioelectron.*, 2017, **87**, 693–700.

38 Y. Upadhyay, S. Bothra, R. Kumar and S. K. Sahoo, *Colloids Surf., B*, 2020, **185**, 110624.

39 K. Abha, I. Sumithra, S. Suji, R. Anjana, J. A. Devi, J. Nebu, G. Lekha, R. Aparna and S. George, *Anal. Bioanal. Chem.*, 2020, **412**, 5671–5681.

40 H.-H. Deng, K.-Y. Huang, S.-B. He, L.-P. Xue, H.-P. Peng, D.-J. Zha, W.-M. Sun, X.-H. Xia and W. Chen, *Anal. Chem.*, 2019, **92**, 2019–2026.

41 R. Tu, B. Liu, Z. Wang, D. Gao, F. Wang, Q. Fang and Z. Zhang, *Anal. Chem.*, 2008, **80**(9), 3458–3465.

42 G. Granados-Oliveros, B. S. G. Pineros and F. G. O. Calderon, *J. Mol. Struct.*, 2022, **1254**, 132293.

43 Y. Wang, L. Dong, R. Xiong and A. Hu, *J. Mater. Chem. C*, 2013, **1**, 7731–7735.

44 F. Zhang, Y. Liu, P. Ma, S. Tao, Y. Sun, X. Wang and D. Song, *Talanta*, 2019, **204**, 13–19.

45 S. K. Sahoo, *New J. Chem.*, 2021, **45**, 8874–8897.

46 Y. Upadhyay, R. Kumar and S. K. Sahoo, *ACS Sustainable Chem. Eng.*, 2020, **8**, 4107–4113.